Wind Turbine EMI Measurement

Uncertainty assessment

S&T
Olof Palmestraat 14
P.O. Box 608
2600 AP, Delft
The Netherlands

Contents

Document Change Record

Version	Date	Prepared by	Change Description
Draft	7 May 2019		Draft version
1.0	21 October 2019		Released
1.1	29 October 2019		Updated Section 4 with respect to the method and result of computing the quantitative impact
1.2	12 November 2019		Updates after ASTRON and AT review remarks: • Section 2.3: Removed sentence under **Terrestrial RFI** referring to "figure below" and removed figure 7. • Section 2.4: Updated text under **ADC resolution** ("SNR" has become "dynamic range" and part of the last sentence has been removed. • Section 2.5.3: Updated text under **Distance proportionality** ("x=1" has become "x=2"). • Updates according **review remarks** in email of , Re: Word versie Eindrappport v1.1., dated Tue 05/11/2019 23:12 • Added **uncertainty of the summation of H-pol and V-pol** and its influence of the separate uncertainties in H and V.
1.2 Final	19 November 2019		Final version: • Removed green highlighting from section 3.6 • Removed review comments • No further substantive changes to version 1.2

1 Introduction

1.1 Purpose and scope

This document describes and justifies the estimation of the uncertainty in the determination of the electro-magnetic interference of a wind turbine generator on the LOFAR antennas.

1.2 List of terms and acronyms

Term/Acronym	Description
ASTRON	Netherlands Institute for Radio Astronomy
EMI	Electro Magnetic Interference
HDF	Hierarchical Data Format
LOFAR	LOw Frequency ARray
S&T	Science and Technology corporation
WTEM	Wind Turbine EMI Measurement
WTG	Wind Turbine Generator

1.3 Reference documents

Documents containing supporting and background information relevant to this document.

Ref.	Title
RD1	NPL Certificate of Calibration 2018100058
RD2	Schwarzbeck Mess-Electronik: VHF-UHF Balun/Holder UBAA9114 with Biconical Elements BBUK9139
RD3	Calibrator_Temperature_Call_test
RD4	TRV-102D Temperature Transmitter Instruction Manual
RD5	DARE Calibration and Reference source FAT
RD6	Calibration_Voltage_Test.xlsx
RD7	Att_CalData.xlsx
RD8	Additional_Simulations_Hoogwerker_V3.pdf
RD9	J. Grifoen, G. Klaver and W.E. Westerhoff, Feb 2016 Netherlands Journal of Geosciences
RD10	https://www.energy-pedia.com/news/netherlands/northern-petroleum-starts-production-from-the-geesbrug-gas-field
RD11	NEO-M8P DataSheet
RD12	DARE Azimuth_freq-list
RD13	DARE H-pol antenne sim_V2

Ref.	Title
RD14	Method for measuring the EMI radiation of wind turbines in relation to the LOFAR radio telescope
RD15	ST-WDMO-WTEM-TN-001-v1.0 Fresnel Zone Analysis
RD16	Cobalt: A GPU-based correlator and beamformer for LOFAR
RD17	WTEM Memorandum: L-formula
RD18	Surveying document of foundation R.02.1
RD19	Email trail: Thu 11/10/2019 16:30, RE: H-polarization simulation and Azimuth simulation in H-polarization,
RD20	Email trail: Thu 17/10/2019 12:43, RE: flux estimation module,

2 Contributing elements

2.1 Overview

In order to determine an estimate of the uncertainty of the measured interference level of the wind turbine, let's look at the main factors that contribute to this determination.

1. Transmission
    a. Reference Source and
    b. Wind turbine
2. Environment (Other RFI sources and propagation and other influences)
3. Reception (LOFAR)
4. Calculations and data processing

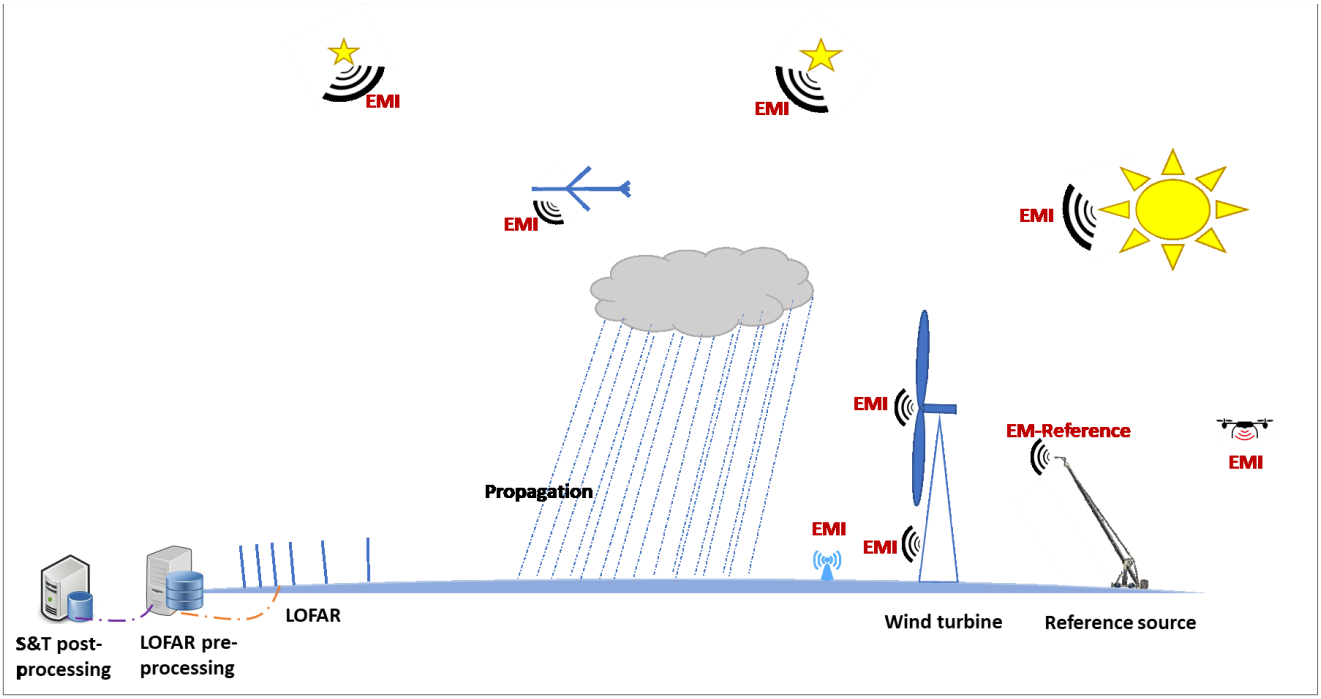

Figure 1: Contributing factors to uncertainty in the measurement of the interference

2.2 Transmission

2.2.1 Reference source

2.2.1.1 Antenna

LAT/LON

Measured accurately with DGPS

The DGPS system has a precision of 0.025m + 1ppm CEP [RD11]. The logged values also include the precision of each record. This value is two orders of magnitude within the resolution elements of the measurement, and can be omitted with high confidence.

The crane has been measured to sway over the course of the measurements, with the magnitude varying with wind strength and direction. Most measurements this sway was limited to <0.01m, however, the worst case (Tuesday 10th, LBA) had a standard deviation of 0.77m.

DGPS position offset

Measured by hand (5.250 ± 0.005 m)

The distance between the DGPS antenna to the reference source antenna. The length of this is measured

by hand and can be considered accurate to ±5 mm. This is substantially smaller than the other spatial errors discussed herein, and can be neglected.

Height

Relative measurement with DGPS, using ground calibration

As above, the height obtained by the DGPS has a precision of 0.025m. This is over 100 time smaller than is resolvable using LOFAR in this geometric configuration.

Direction

H-polarization: antenna and beam roughly directed at SUPERTERP in the LOFAR core.

V-polarization: antenna and beam omnidirectional in the horizontal plane, aligned approximately to direction of the SUPERTERP (90° from H-polarization direction)

The crane azimuth is set rather coarsely, however, a much more accurate value of this direction can be calculated. This is done using the DGPS position of the base of the crane, and forming a known triangle with the DGPS and reference source antennae. This does rely on the assumption that the beam is completely rigid relative to the crane. The scale of the variation in direction is now inferred from the stability of the DGPS LAT/LONG position discussed above. Even in the worst measured case, when the sway was largest, the influence this had on the orientation was determined to be small enough to have no significant influence on the orientation of the beam pattern.

The field strength as a function of azimuth over the ±17° angular width of the LOFAR core, is shown to be consistently within 0.2dB for the vertical polarisation [RD1], or 1.0dB for the horizontal polarisation [RD12].

It was discussed amongst the parties as to whether or not a NPL calibration was also necessary for measurements in the horizontal polarisation. Based on [RD12] it was agreed with AT [RD19] that a calibration for horizontal polarisation is necessary. Below a recap of the email trail in [RD19].

Recap from email trail [RD19] (in Dutch)

Donderdag 12 September 2019 17:18, (S&T)

Beste

Bijgaand vind je de twee gevraagde rapporten m.b.t.:

- H-polarization simulation (nav discussie over wel/niet kalibratie van de referentiebron in de H-polarisatierichting)
- Azimuth simulation in H-polarization (het simuleren van het effect van de H-polarisatierichting in verschillende hoeken)

Donderdag 10 Oktober 2019 15:05, (S&T)

Hallo

Eerder heb ik de gevraagde simulaties door DARE aan ieder opgestuurd. Volgens mij heb ik niet terug gehoord wat jullie conclusie hieruit is. De invloed lijkt gering genoeg, maar ik zie dat graag door jullie bevestigd.

Donderdag 10 Oktober 2019 15:05, (AT)

Beste

Ik vermoed dat ik hierop gereageerd heb tijdens onze nabespreking van de meetsessie op 25 sept en dat het in het verslag daarvan te vinden moet zijn, en inderdaad niet in een rechtstreeks mailtje.

Want ik had er wel naar gekeken en zelfs met collega's over gesproken. De essentie was dat de simulaties inderdaad voldoende vertrouwen geven en onze aanname ondersteunen nl. dat de kraan niet een zodanige invloed heeft op het antennepatroon bij de H-pol metingen dat her-kalibratie nodig is.

Antenna gain

The antenna has a frequency dependent gain, which is documented in the manual

The antenna has been provided with detailed documentation of its performance [RD2] and its gain as a function of frequency is shown below. The effect of this on the transmitted signal is detailed in [RD1, RD5].

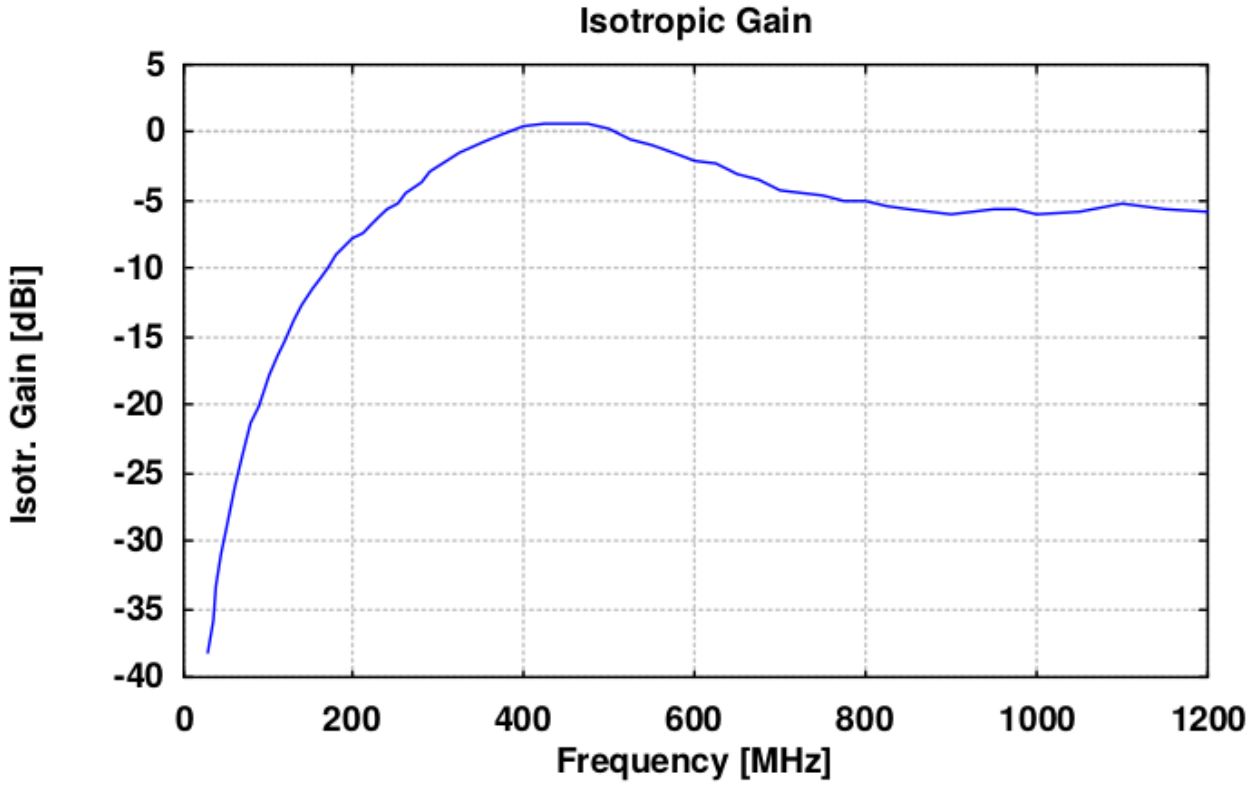

Figure 2: Antenna gain

2.2.1.2 Source Calibration

Temperature

Effects the power output (calibration file)

The temperature dependence has been shown to be within ±0.2 dB within an operating range of 5-45°C as shown below [RD3, RD4, and RD5]. The result of this effect can be merged into the L formula calculation.

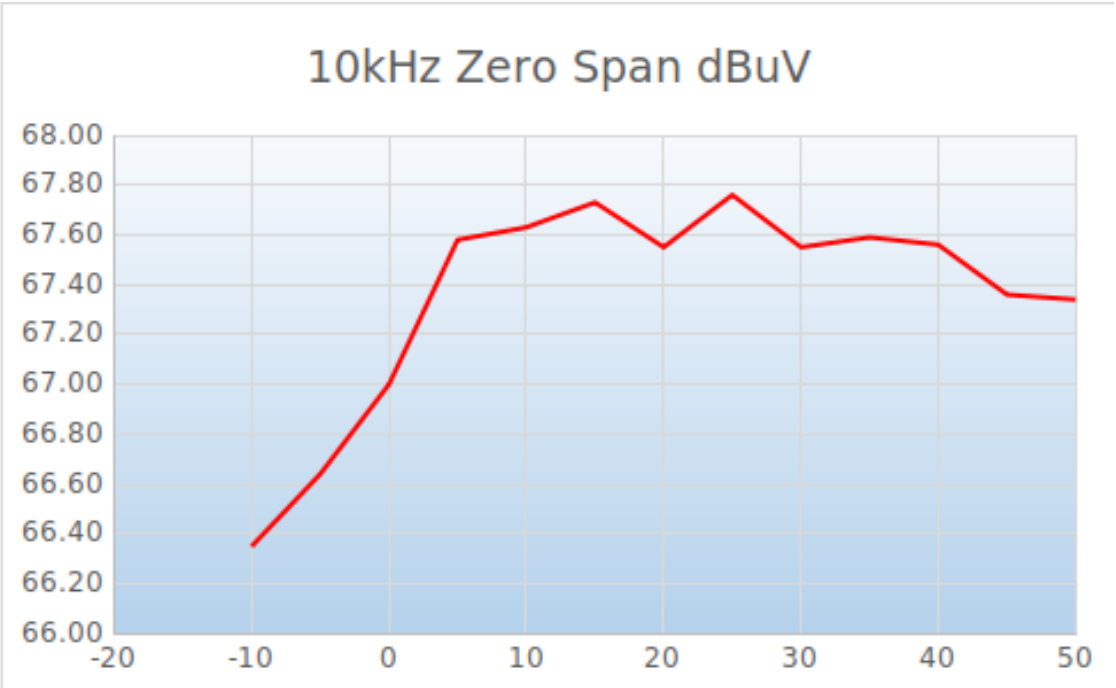

Figure 3: Temperature dependence of the calibration source output

V-battery

Effects the power output, (calibration file)

The effect of battery voltage on signal output is detailed in [RD6]. It is shown that for the 30MHz end of the spectrum the power ranges over 0.25 dB, whilst at the 240MHz end, this range is 1.40 dB. The figure below shows that output quickly becomes unreliable below 11V, and this data is consequently discarded from processing.

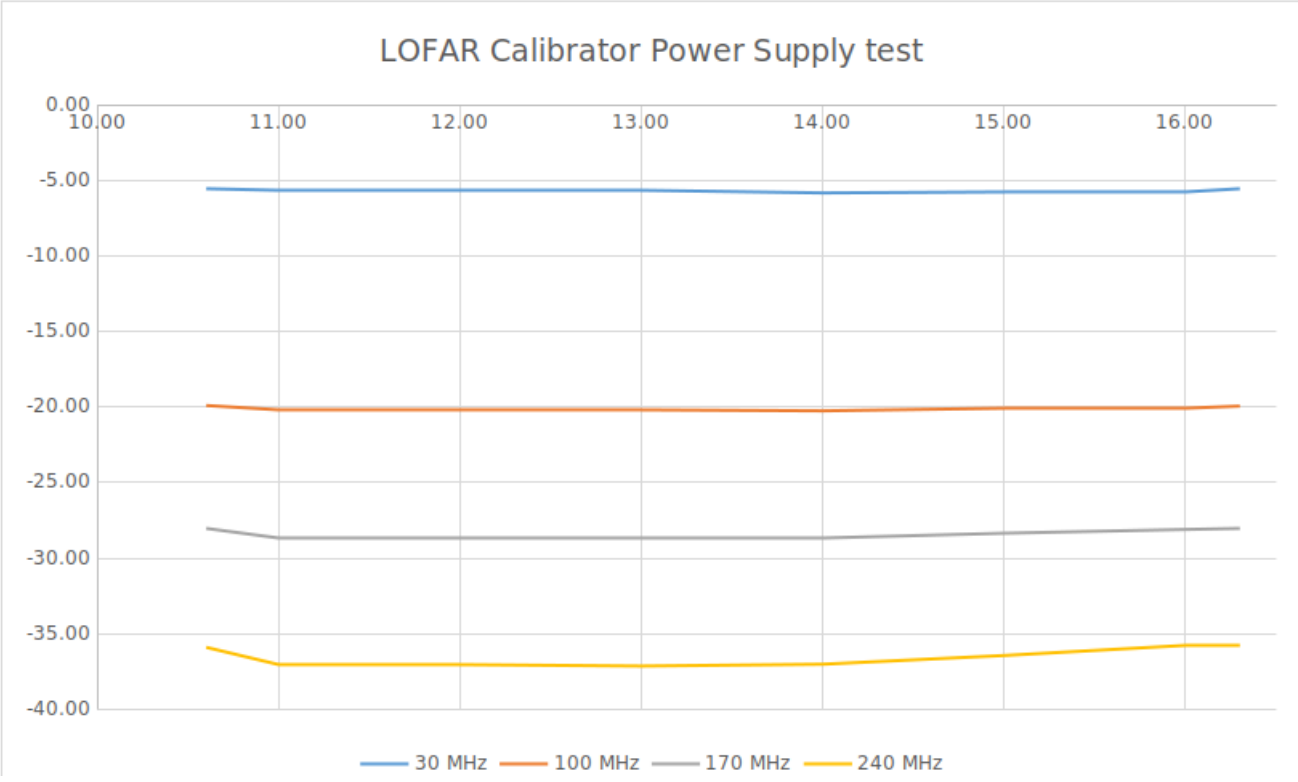

Figure 4: Battery voltage dependency of the resource output

Attenuator

Effects the power output, (calibration file)

The spectral response of the attenuator has been measured by DARE and is found in [RD7]. The -35dB response is shown below to be slowly varying and stay within 0.14dB of the intended -35dB level. This component was not used for this measurement campaign, but is still included here for completeness.

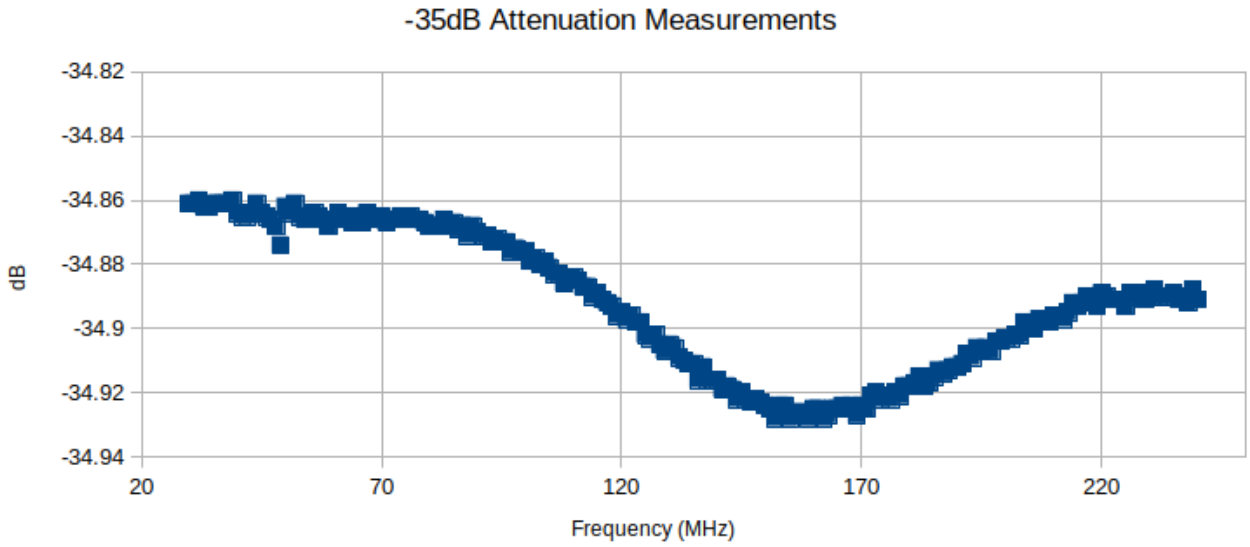

Figure 5: Attenuator dependency of the resource output at -35 dB

Power (NPL)

Power calibrated at NPL (calibration file)

The NPL power calibration show the over the air tests are within ±1.5dB [RD1].

Amplifier gain

The amplifier gain is part of the Power calibration (NPL, see row above), and doesn't need to be considered separately.

2.2.1.3 Crane

Crane EM properties

Influence of crane structure on measurements

1. V-polarization
2. H-polarization

Dare originally performed simulations of the interaction between the broadcast signal and the upper 15m of the crane structure for the *vertically* polarised measurements [RD8].

The construction option that was chosen, rotating the mast 90 degrees in Z-plane with the antenna at 5.25 meter from the crane (section 3.1 [RD8]) was concluded to have a peak-peak variation is 2.4 dB, leading to an uncertainty of ±1.2dB for V-polarisation.

This process was later repeated for the *horizontally* polarised configuration [RD13]. These simulations predicted a frequency dependant variation of gain, due to resonances and reflections, to a peak-peak gain deviation, between 30 and 240 MHz, of 5.1dB, leading to an uncertainty of ±2.55dB for H-polarisation.

Elevation differential between the reference source and WTG

The reference source is at different elevation than the nacelle, resulting in a different altitude angle at the point of measurement.

The reference source is at lower elevation (100m) than the nacelle (145m), which is a likely source of RFI due to the equipment located within.
The reference source height is taken to be equal to the relevant height as defined in "Artikel 1" of the covenant. Attached to this height is a specific antenna gain for the LOFAR antennas. This antenna gain varies rather strongly as a function of altitude. Because of this complication, the covenant parties later agreed in a CoCom that the limit (when measured with LOFAR) applies to the product of the WTG emission and the antenna gain, fixed by calibration at 100 m altitude. (Given that the entire structure is 209 m tall, this is half-way the WTG as a whole). This agreement ensures that what is actually measured is proportional to how much it affects LOFAR. Emission from the base of the WTG will appear fainter than it actually is, while emission from above this point appears stronger.

2.2.2 Wind turbine

Reflections

The WTG may reflect reference source signals, or other RFI signals.

Some evidence of external reflections by the WTG has been found in the measurement data. This is discussed in detail in the full report. Regarding their effect on the measurement uncertainties, it isn't possible to effectively separate out power from different origins, only to determine the direction the received power comes from, and to treat it in its entirety.

Refractions

The WTG will be relatively close to the reference source signal.

Fresnel analysis has been performed to obtain an estimate how in how much the WTG affects the reference source value [RD15]. This has verified that the WTG is not within the first Fresnel Zone for any of the antenna used in the measurements.

Position accuracy

The position accuracy might be different from the intended position

The construction position of the WTG has been measured using Total Station [RD18]. This value comes with a precision of ± 1mm in x and y, and 0.1mm in z.

2.3 Environment

Celestial source interference

Celestial sources not subtracted, or with unexpected artefacts

The pre-processed data arriving from ASTRON has dominating celestial sources pre-subtracted. That turns out to be all sources for which the combined PSF side lobes due to their apparent flux density might lead to a noise floor that makes measuring a WTG at the -35 dB level impossible (ideally 10 dB lower).

Only the brightest few sources are removed, including Cassiopeia A, Cygnus A, Hercules A, and Taurus A. All remaining celestial sources will contribute to the measurement noise level.

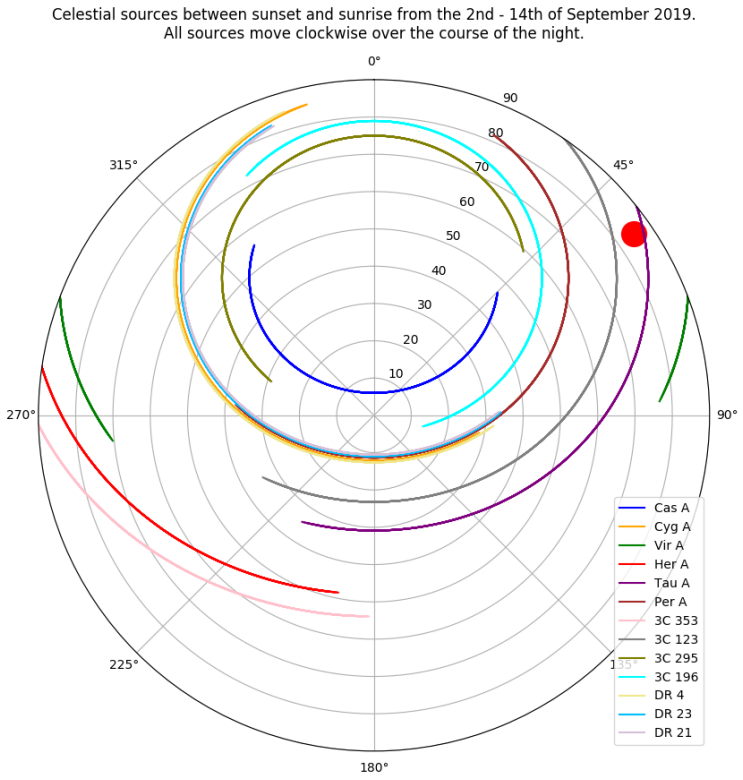

Figure 6: Celestial sources between sunset and sunrise 2nd and 14th of September 2019

To prevent any interference from the active solar surface, all observations are performed at night.

As a result of our investigations into the noise present in the data, it was discovered that even after these sources had been subtracted some significant fringe patterns remained in the sky-plane images. Through intensive analysis, it was determined that these were artefacts due to very short projected baselines approximately aligned with the brightest celestial sources. Short baselines are now suppressed in order to mitigate this phenomenon.

Terrestrial RFI

Terrestrial RFI may be contributed either to the Reference Source or to the WTG or both).

Terrestrial RFI has turned out to be a larger problem than anticipated. It is generally expected that rural Drenthe should be radio quieter than the national average, however, this assumption can't be counted on.

AT and ASTRON monitored the background noise level in the vicinity of the tests throughout the measurement period. Some sources have been identified and dealt with on a case by case basis. These included a nearby outdoor theatrical production (monitored and measured and found to be below the level of concern in the bands of interest), and a faulty power interface connecting LOFAR to the power grid (adjacent station omitted from further analysis).

Propagation effects, T, Humidity, Rain, soil moisture, reflections

Propagation effects will impact the reference source signals in a similar way as the WTG signals. The impact on the measurements and comparison will therefore likely to be small.

Each of these phenomena will affect the signal from the reference source and the signal from the WTG almost equivalently. There is less than 5% difference in the path length, and less than 6° angular difference between their respective lines of sight. This difference is much too small for to have any substantive effect on the received signal.

Local geological stability

Changes in the antenna positions due to subsidence will be small (at most a cm a year.

The region of the windfarm and LOFAR occupy the same tectonic environment, with no known faults in their vicinity [RD9]. They also sit on the same geological structure, being a plane of Aeolian cover sand [RD9]. Consequently, it is incredibly unlikely that any substantial natural ground movement. There are also no gas or oil resources being exploited in the immediate region of interest, removing the other most likely cause of geological instability [RD10].

2.4 LOFAR Reception

The LOFAR "receiver" elements of uncertainty include:

- Station response
- Antenna response
- Thermal noise
- Phase noise
- ADC resolution
- Antenna positions within station
- Phase centres of each station

Station response

The station response is not completely known, especially not for the lower elevation angles that are being used. As the reference source signal is well characterized (calibrated by NPL) , the source can be used to measure the the gain vs frequency response of the station for an elevation angle corresponding to the reference source at 100 m positioned at the "gebroken lijn" parking place more-or-less north of the WTG. Note as the comb-spacing of the source is 1 MHz, there is a need to interpolate the response function for those channels for which no comb signal is available. Thus, as the station response is by-design measured at the relevant height (as mentioned in Artikel 1 of the covenant) the station response is no source of uncertainty for the measurement interpretation.

Antenna response

Antenna response for these low elevation angles is not known. There might be some difference antenna gain for signals coming from the reference source and signals coming from the various heights of the WTG.

Measurements have been conducted by ASTRON to measure antenna gain at these lower elevation angles. This is wrapped into the gains described above.

Thermal noise

Thermal noise; Worst case SEFD of the LOFAR system has been estimated at 3.5 Jy [lofar-as-a-measurement-device, 2018].

It has been derived that approximately 80 seconds of integration will be sufficient to come to a thermal noise sufficient for measuring the -35 dB level. (The structural noise will be covered by the source subtraction).

Phase noise

The timing equipment will be less than ideal although a GPS conditioned Rubidium clock is being used.

In practice this has not demonstrated any substantive influence on the results. It is therefore, considered to be negligible for the purposes of this project.

ADC resolution

Typically, the formula SNR = 6.02N + 1.76dB[1] (with N =the number of bits) is used to determine the effect of the quantization noise by the ADC (assuming the full bandwidth is used in the processing; and it is).

N = 12 bits: The dynamic range = 74 dB.

This influence can be disregarded.

Antenna positions

The antenna positions need to be known to perform the phase corrections

The antenna positions have only been measured when LOFAR was initially deployed in 2009. These positions are updated annually to account for continental drift, however, are not re-measured.

Accumulated errors are estimated to be within ±0.1m for each individual antenna.

Phase centre positions

The phase centres are being used for the phase corrections.

Similarly, to the previous point, the phase centres have not been re-measured since the time of LOFAR's commissioning in 2009, but have been updated for continental drift each year. The uncertainties on the phase centres are an average of the positions of the antennae, so have a better precision of ±0.03m. This is many times smaller than the shortest wavelength used by LOFAR (1.2m), so can be comfortably disregarded.

2.5 Calculation

2.5.1 Pre-processing at ASTRON

These items are based on work performed by ASTRON on data before it is received by S&T. Verification of these points has required some inputs from ASTRON.

Correlator

On the critical path in the LOFAR data analysis chain. It is expected that this has been subject to thorough review and should be unlikely to introduce any issues.

The correlator used during this project is known as COBALT2.0 [RD16] and has been commissioned through to 2018. This correlator has been thoroughly tested through ASTRON's own internal exacting assessment, and also been put up to international scrutiny, and has found to satisfactorily meet its requirements [RD16].

Source Subtraction

This is similarly a normal part of regular LOFAR processing in which celestial sources brighter than the source of interest are subtracted using existing models of the object's on-sky geometry.

Celestial source subtraction turned out to be a much more difficult problem than initially anticipated. This was largely a consequence of observing at such a low elevation angle, where LOFAR has not had much observing experience. In each of the measurement campaigns, this step ended up requiring multiple iterations in order to sufficiently and effectively suppress the bright sources dominating the data.

In the end we have had to remove up to four sources, as well as supress all baselines shorter than 60 times the wavelength (600m at 30MHz, 72m at 250MHz).

---

[1] Here we are ignoring the measured signal to noise ratio and distortion to derive the effective number of bits. *See:* https://www.analog.com/media/en/training-seminars/tutorials/MT-001.pdf

Each additional source subtracted does remove information from the system, which included power from the WTG direction. Therefore, minimising this number is important for maximising the achievable SNR.

Filtering

Another standard LOFAR process. This is not performed on narrow band 3 channel data, used for detecting the reference source

Filtering has shown itself to provide a substantial improvement to the noise floor for the wideband datasets. Measurement uncertainty is, therefore, significantly reduced to effective flagging.
Over-flagging has the potential to reduce the signal strength, and under-flagging can prevent the omission of unwanted RFI. However, we have seen no evidence of either of these issues in the data analysed.

Calibration

It is was initially uncertain if there are any prior gain (or otherwise) calibrations in the data. These could have been at the antenna, station, or array level, or in any pre-processing.

ASTRON has confirmed that there are no additional calibration steps in their pre-processing. The only steps that affect the intensity or phase in the data are necessary functional processes, such as correlation, source subtraction, and averaging. There is therefore no additional impact on uncertainty here.

2.5.2 Pre-processing at S&T

These processes are performed by S&T with tools developed by S&T.

Data Conversion

Data arrives from ASTRON in a CASACORE format. This is converted to the more standard HDF5.

Input and output quantities have been verified to match to machine precision.

Splitting by mode

The data is divided depending on the observation mode at the time it was acquired using reference source log-files.

Input and output quantities have been verified to match to machine precision.

The splitting process has been verified to split exactly where intended. A limited example of this for a specific frequency (78MHz) and short timeframe is shown in the following diagram.

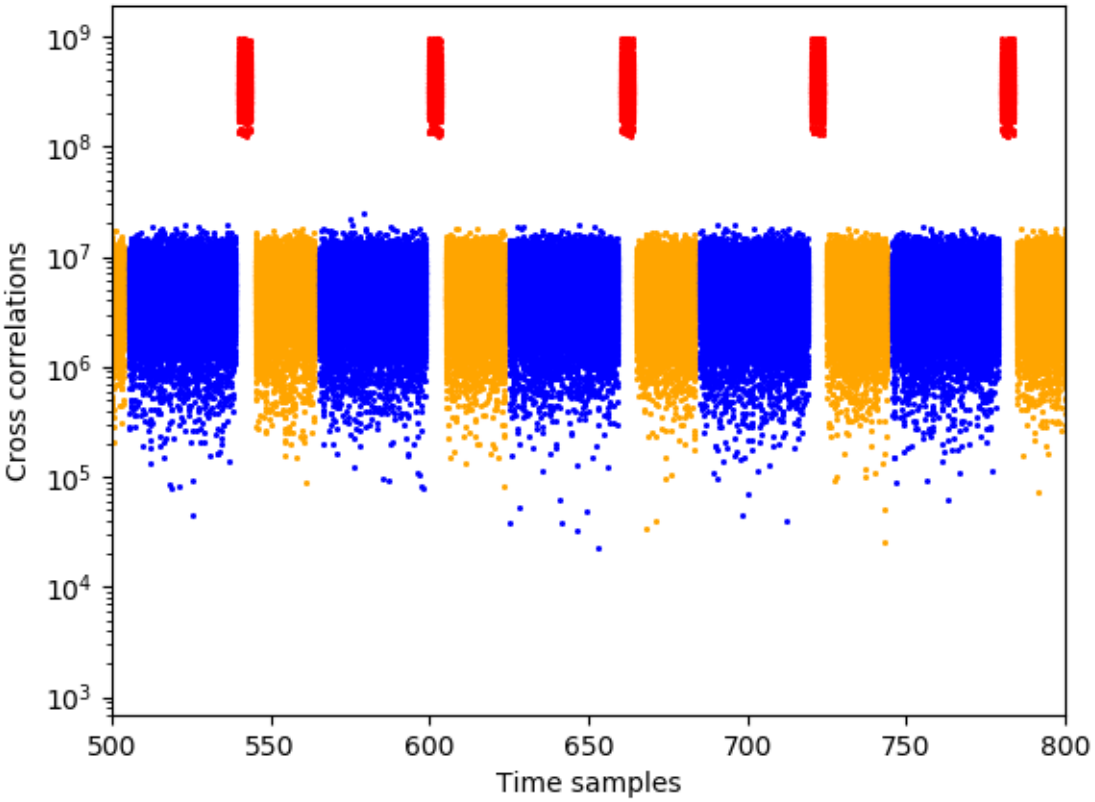

Figure 7: Limited example of splitting process for 78MHz and a short timeframe

2.5.3 Calibration at S&T

These processes are performed by S&T with tools developed by S&T.

Phase Calibration

Phase calibration is a necessary step in order to obtain sensible images.

The phase calibration process has developed in many stages over the course of this project. With iterations often taking inputs from ASTRON and AT. The final process being used has been accepted with confidence by all parties as functioning correctly. This calibration step lowers the noise floor and increases the relative signal strength improving the SNR. It does not affect the uncertainties directly, but only through its influence on the ACM, and is therefore accounted for in the analysis of the generated images.

Amplitude Calibration

Amplitude calibration may prove to be necessary, but has the potential to introduce some DC offsets.

In the end phase calibration has proven to be sufficient, and amplitude calibration has not been used. When it was tried it tended to cause artefacts due to over fitting, so it wasn't able to be robustly relied upon.

Distance proportionality

The relationship between intensity and distance (1/(d^x)) is affected due to propagation effects close to the ground. This will need to be determined for gain calibration to be effective.

This question was resolved by fitting the intensities in the observed data to with a power law, resulting in x=2, which was subsequently verified to be backed up by the physics of EM propagation. In an email discussion [RD20] it has been agreed that the error made here introduces an uncertainty of ±0.26 dB. Below a recap of the email trail in [RD20].

Recap from email trail [RD20] (in Dutch)

[S&T]

Het gaat om de afstand verschillen binnen de WTG cube, en

niet tussen de afstand verschil tussen de twee kubussen.

Binnen de kubus leidt dat toe (200x200x250) dus center <—> hoekpunt is 160m:

20*math.log10(4500) - 20*math.log10(4500-160)

0.31 dB

Verder wordt voor de WTG alleen het maximum in een beam rond de windmolen

gebruikt met dimensies 50m x 50m x 250m.

Daar is de afstand maximaal 135m van af de cube center.

0.26 dB

Maar in praktijk zit de z waardes altijd zo rond de cube center,

dus voor de L-waarden licht die nog een stuk lager

[AT]

Inhoudelijk eens

[AT]

Ik kan me ook in deze benadering vinden,

en laten we inderdaad vanmiddag proberen af te tikken.

Het is wel + en - .31 of .26 dB toch.

(ASTRON) has confirmed, in a conference call of 18 October, that this explanation is valid.

Bandwidth

The data was originally expected to be a broadband source observed in 50kHz bins. Since the adoption of the 1MHz carrier spacing, this no longer makes sense. The relationship between the bandwidth and the gain needs to be established

In the pre-processing performed by ASTRON, the spectral averaging to 14 channels (42 kHz), was chosen partly in order to account for the difference in bandwidth with the 3 channel (10 kHz) calibration data.

This has no numerical consequence on the resultant uncertainty, only to remark that is has been taken into account.

Outlier filtering

Some basic filtering is applied to the data to remove clear outliers (5 sigma).

This filtering has been demonstrated to effectively remove some remaining outliers which remained after ASTRON's filtering, consequently reducing the noise floor. This step was also adapted to remove the large values found within the data after the last iteration of the pre-processing and source subtraction by ASTRON. The overall effect on the uncertainties is again wrapped into the masked ACMs, by reducing the number of available baselines for imaging, by increasing the number masked elements.

2.5.4 Imaging at S&T

These processes are performed by S&T with tools developed by S&T.

Imaging algorithm effectiveness

The S&T developed near field imaging algorithm has been developed with a known calibration source assumed to be in place. The expected results for other situations are less clear and need to be determined.

The imaging algorithm has been demonstrated to successfully discern the reference source, as a good approximation of a point source. That is a single, simple, free-floating, point-like shape.

The WTG, on the other hand, is expected to have a more complex geometry than this. This geometric shape does not simply appear in the generated images. Instead, we see a convolution of this geometry, and the point source response function of the experiment (often called the point spread function). Mathematically undoing this convolution is not a trivial operation, fortunately, we have not seen any overwhelming evidence of much actual structure within the WTG images, where there was a notable detection.

The resultant effect of this discrepancy on the uncertainties is that the maximum pixel is no longer a viable proxy for the source intensity as it was with the point source. Based on the point-like behaviour observed in the generated images, a 'worst-case' uncertainty can be estimated. If this situation is assumed to be two unresolved (overlapping) discrete sources with similar intensities, then an error of 3dB is sufficient to cover this discrepancy.

H-pol and V-pol summation

The measurements have shown that the antennas are positioned such that the antenna YY-polarization is *mainly* affected by the H-polarization component of the reference source signal, and the antenna XX-polarization is *mainly* affected by the V-polarization component of the reference source signal. The summation of the H-pol and V-pol data now has been implemented by taking YY-antenna-data only for the H-pol and the XX-antenna-data only for the V-pol, although we are neglecting some part of the signal for both the H-pol and the V-pol measurements.

It has been estimated that the error is at most 1 dB.

Absolute vs relative calibration

By making use of the absolutely calibrated reference source makes it possible to measure the emission of the WTG in absolute terms.

3 Combining Uncertainties

This section combines the uncertainties from section 2 with the error propagation in the L-formula. The approach will be as follows, first derive the L formula in its non-logarithmic form, then apply the Error Propagation formula and try to capture all the (stochastic) error components within the L formula.

3.1 L formula in normal form

The L formula such as described in [RD14, 17] expresses the ratio of the WTG Power P_w over the norm P_{norm}.

$$L = \frac{P_w}{P_{norm}}$$

Where P_{norm} is defined as the standard EMC norm EN55011 value $50\ dB\mu V/m$, as can be found in Chapter 6 in RD[14]. Meanwhile [RD17] gives use the complete L-formula updated to suite the current measurement approach as

$$L = P_{cal} - 10\log_{10} B + 10\log_{10} {WD_w}^2 - 10\log_{10} {CD_c}^2 + 0.8$$

The power of the WTG can't be determined directly from the voxel cubes. To this end we determine P_w by relating the flux densities measured on the WTG (W) to the flux densities at the Calibrated Reference Source (C) with known intrinsic power P_{cal}.

The flux density of the WTG and calibration source are related through the value of P_{cal}, through their relation in the distance;

$$P_w = P_{cal} * \frac{W\ D_w^n}{C\ D_c^n}$$

Where D_w and D_c are respectively the distance from the LOFAR phase centre to the WTG and the calibration source. The index n expresses the inverse distance relation with n=2 in the far-field and n=1 in the near field.

The L-formula in normal form then becomes;

$$L = \frac{P_{cal} W D_w^n}{P_{norm} C\ D_c^n}$$

From the above equation, the relative error propagation can be provided;

$$\left(\frac{\sigma_L}{L}\right)^2 = \left(\frac{\sigma_{P_{cal}}}{P_{cal}}\right)^2 + \left(\frac{\sigma_W}{W}\right)^2 + \left(\frac{\sigma_{D_w}}{D_w}\right)^2 + \left(\frac{\sigma_C}{C}\right)^2 + \left(\frac{\sigma_{D_c}}{D_c}\right)^2$$

Here σ_x is the estimated or measured uncertainty within the given variable x. This equation will be simplified later on as for example the uncertainty within the windmill distance will be negligible. The uncertainties of the measured flux densities σ_W and σ_C will be estimated directly from the environment noise. The uncertainty within the calibration source and the other components will be modelled within the next sections.

3.2 Calibration Power Uncertainty

The power, P_{cal} has been calibrated to the P_{norm} as described in section 2.2.1. These values are provided in RD [5] and depend on frequency f, giving us $P_{NPL}(f)$.

Furthermore, P_{cal} was measured to be also a function of Temperature (T), Battery Voltage (B) and angles θ, φ, see section 2.2.1. These correction factors can be included in the following way and for a given time t we have the following equation;

$$P_{cal}(f, T, B, \theta, \varphi; t) = P_{NPL}(f)\ C\big(T(t)\big)\ C(B(f,t))\ C(\theta, \varphi)$$

Here the functions $C(x)$ are the relative correction factors as measured within the lab.

For the moment, we will ignore the angular dependency, since it requires a more complicated model as it needs to be modelled for all the LOFAR stations independently and also depends on the geometric accuracy

with which the calibration source is aligned.

The temperature and Battery Voltage are functions of time and need to be measured during the observation window. So, the time averaged value for P_{cal} then becomes;

$$P_{cal} = P_{NPL}(f) < C\big(T(t)\big)\, C(B(f,t)) >,$$

where <> is the time averaged value. This results in the conclusion that for the above equation the main uncertainties within P_{cal} comes from the measurement errors in $P_{NPL}(f)$. Since the time-average values will have a reduced value of $1/\sqrt{N_{samples}}$ where $N_{samples}$ is approximately of the order of a thousand.

Note that this assumes that the errors are independent, systematic errors may still need be included.

3.2.1 Uncertainty of calibration input parameters

The uncertainties for these parameters is summarised below and is taken directly from their relevant documentation.

Table 1: Uncertainty of calibration input parameters

Parameter	Uncertainty	Percentage	Reference
$P_{NPL}(f)$	± 1.5 dB	4.0032	RD1
$\big(T(t)\big)$	± 0.4 °C	2.0	RD4
$(B(f,t))$	± 0.01 V	0.04	RD6

It is therefore possible to determine $\sigma_{P_{cal}}$ using percentage uncertainties as follows

$$\frac{\sigma_{P_{cal}}}{P_{cal}} = \left(\frac{\sigma_{P_{NPL}}}{P_{NPL}}\right) + \left(\frac{\sigma_T}{T}\right) + \left(\frac{\sigma_B}{B}\right)$$

yielding a static percentage uncertainty of 6.25% for P_{cal}.

3.3 Distance Uncertainties

This section will describe the distance uncertainties factor within the L-formula. These uncertainties are approximated using the radial size of the point-cloud for each band.

This physical distance from LOFAR to both the WTG and the reference source is known to better than 0.001%, based on the precisions described in Section 2. These are orders of magnitude smaller than the resolution limited dispersion in the point-cloud images, and can be safely ignored. The reference source in practice has a different distance for the horizontal polarised measurements, than it does for the vertical, however this difference is small enough to be ignored. The calculated values are treated as static and are shown as follows:

D_w	4255m
D_c	4485m

As an example, the point clouds for the 12th of September LBA observations are shown below. The reference source is on the left, and the WTG is on the right. The radial extent of the point cloud for the reference source is 12m, whilst for the WTG it is 55m (to two significant figures).

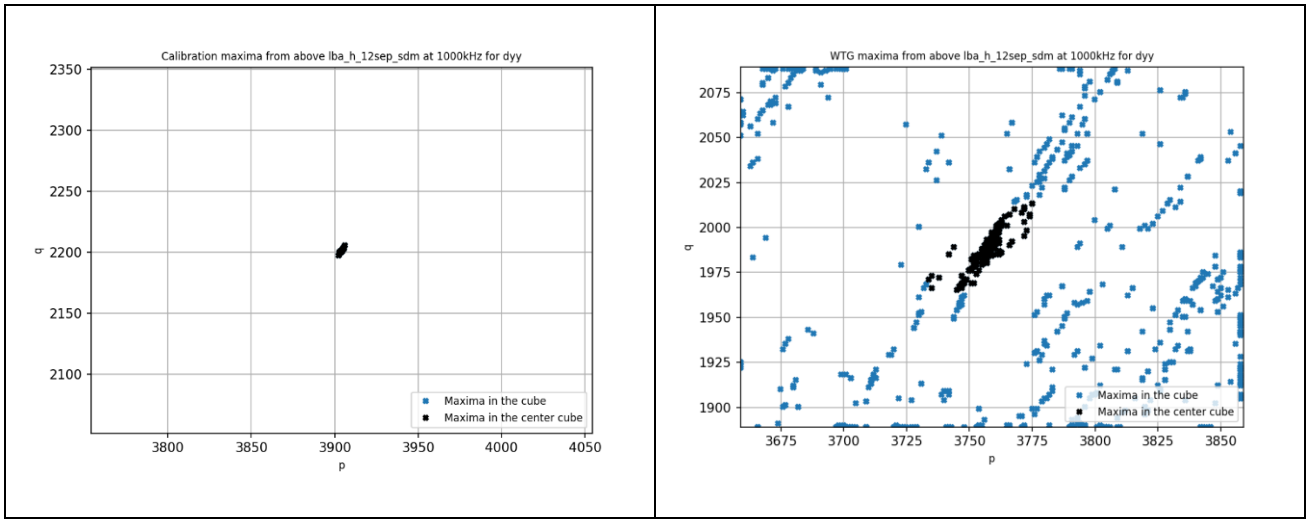

Figure 8: Point clouds 12th September LBA observations. Reference source left, WTG right

This results in the following:

$$\frac{\sigma_{D_w}}{D_w} = \frac{55}{4255} = 1.3\%$$

$$\frac{\sigma_{D_c}}{D_c} = \frac{12}{4485} = 0.27\%$$

These values need to be determined for each band, and are expected to generally scale approximately with wavelength.

3.4 Flux density uncertainties

This section will include the flux measurement uncertainties, σ_W and σ_c . A viable estimate of these values can be taken from the RMS of the OFF measurements. This must be done separately for each averaged spectral band. The flux density values themselves come from the measured signal level, leaving us with an approximate inverse of the SNR.

These values also need to be taken separately for each averaged spectral band.

3.5 Summation H-pol and V-pol

Using only the XX-component of the antenna data as the V-pol component, and only the YY-component of the antenna data as the H-pol component will introduce an estimated uncertainty of 1 dB per polarisation. The uncertainties for these separate polarisation values are then combined in quadrature.

3.6 Error estimate of L within the Test measurements

The total relative error per polarisation as stated above is given by,

$$\left(\frac{\sigma_L}{L}\right)^2 = \left(\frac{\sigma_{P_{cal}}}{P_{cal}}\right)^2 + \left(\frac{\sigma_W}{W}\right)^2 + \left(\frac{\sigma_{D_w}}{D_w}\right)^2 + \left(\frac{\sigma_C}{C}\right)^2 + \left(\frac{\sigma_{D_c}}{D_c}\right)^2$$

With the static components entered this becomes

$$\left(\frac{\sigma_L}{L}\right)^2 = 0.004 + \left(\frac{\sigma_W}{W}\right)^2 + \left(\frac{\sigma_{D_w}}{4255}\right)^2 + \left(\frac{\sigma_C}{C}\right)^2 + \left(\frac{\sigma_{D_c}}{4485}\right)^2$$

Rearranging for σ_L results in,

$$\sigma_L = L\sqrt{0.004 + \left(\frac{\sigma_W}{W}\right)^2 + \left(\frac{\sigma_{D_w}}{4255}\right)^2 + \left(\frac{\sigma_C}{C}\right)^2 + \left(\frac{\sigma_{D_c}}{4485}\right)^2}$$

The remaining seven free parameters are calculated per polarisation in each averaged spectral band, and can in inserted at this point.

The combination of the uncertainties for the two polarisations is also summed in quadrature as follows.

$$\left(\frac{\sigma_{L_{Tot}}}{L_{Tot}}\right)^2 = \left(\frac{\sigma_{L_H}}{L_H}\right)^2 + \left(\frac{\sigma_{L_V}}{L_V}\right)^2$$

4 Quantitative impact summary

The individual element contributions from the detailed exploration of the contributing elements in section 2 in Table 3. Based on the quantitative impact of the summary of the individual contributions, given in Table 2, the total uncertainty in the measurements is estimated at:

V-measurements: ±2.0 dB

H-measurements: ±2.9 dB

V+H-measurements: ±3.3 dB

Similarly, to Section 3.1, these individual dB values must be added in quadrature (section 3.6). This is a consequence of the dB scale being an inherent combination of values as a ratio, rather than an absolute, discrete value of its own.

Table 2: Summary individual element contributions to the measurement uncertainty

Name	Conclusion	Quantitative Impact	
		Vertical polarization	Horizontal polarization
Transmission, Reference source, Antenna			
Direction	Some gain variation across the antenna pattern	±0.2 dB	±1.0 dB
Transmission, Reference source, Source calibration			
Power (NPL)	Third-party calibration measurements of entire spectral range	±1.5 dB	±1.5 dB
Transmission, Reference source, Crane			
Crane EM properties	Simulations predict a spectral variation due to reflections and resonances.	±1.2 dB	±2.55 dB
Calculation, Calibration at S&T			
Distance proportionality	This question was resolved, and determined to have no influence on uncertainties.	±0.26 dB	±0.26 dB
Polarisation leakage	Incomplete coupling between the transmitted polarisation and LOFAR's dipoles.	±1.0 dB	±1.0 dB
	Total	**±2.0 dB**	**±2.9 dB**
	Total H+V	**±3.3 dB**	

Table 3: List of individual element contributions

Name	Conclusion	Quantitative Impact	
		Vertical polarization	Horizontal polarization*
Transmission, Reference source, Antenna			
Lat/Long	Position is accurate to within ±25mm, which is substantially smaller impact than other spatial effects	Negligible	
DGPS position offset	Position is accurate to within ±5mm, which is substantially smaller impact than other spatial effects	Negligible	

Name	Conclusion	Quantitative Impact	
		Vertical polarization	Horizontal polarization*
Height	Position is accurate to within ±25mm, which is substantially smaller impact than other spatial effects	Negligible	
Direction	Some gain variation across the antenna pattern	±0.2 dB	±1.0 dB
Antenna gain	Incorporated into NPL measurement	Nil	
Transmission, Reference source, Source calibration			
Temperature	Temperature dependence has been measured. It is then accounted for in the L-formula calculations. *This impact is not added to the total measurement uncertainty estimation*	±0.2 dB	
V-battery	Battery voltage dependence has been measured. It is then accounted for in the L-formula calculations *This impact is not added to the total measurement uncertainty estimation*	±0.25 dB LBA ±1.4 dB HBA_HIGH	
Attenuator	Not actually used in this measurement campaign	Nil	
Power (NPL)	Third-party calibration measurements of entire spectral range	±1.5 dB	
Amplifier gain	Incorporated into NPL measurement	Nil	
Transmission, Reference source, Crane			
Crane EM properties	Simulations predict a spectral variation due to reflections and resonances.	±1.2 dB	±2.55 dB
Elevation difference (WTG/ref source)	Almost identical propagation path, in spite of elevation difference	As this was agreed, it is part of the measurement definition	
Transmission, Wind turbine			
Reflections	See full report for discussion on possible reflections	N.A.	
Refractions	Fresnel analysis confirmed this is not a dominant issue for the experiment geometry as used.	Negligible	
Position accuracy	Position is accurate to within ±1mm, which is substantially smaller impact than other spatial effects	Negligible	
Environment			
Celestial sources	A few bright sources removed and all short baselines omitted. Remaining sources are part of the background RMS.	RMS	
Terrestrial RFI	Some sources identified and monitored leading to the omission of some specific stations. Remaining sources are part of the background RMS.	RMS	
Propagation effects	Near identical propagation path means near identical influence from environmental phenomenon.	Negligible	
Geological stability	The region of interest can be confidently considered to be static.	Nil	

Name	Conclusion	Quantitative Impact	
		Vertical polarization	Horizontal polarization*
LOFAR Reception			
Station response	Deviation from the ASTRON models is unnecessary	Nil	
Antennae response	Deviation from the ASTRON models is unnecessary	Nil	
Thermal noise	Thermal noise is incorporated into the image RMS.	RMS	
Phase noise	No observable influence detected	Negligible	
ADC resolution	The dynamic range of the 12-bit ADC is sufficient to cope with most RFI. (In fact, the signals we are interested in, are orders of magnitude smaller than the ADC resolution.)	Negligible	
Antennae positions	Measured once in 2009 and updated annually for continental drift. Accurate to within ±100mm which is substantially smaller impact than other spatial effects	Negligible	
Phase centre positions	Measured once in 2009 and updated annually for continental drift. Accurate to within ±30mm which is substantially smaller impact than other spatial effects.	Negligible	
Calculation, Pre-processing at ASTRON			
Correlator	No additional uncertainties are introduced in this step.	Nil	
Source subtraction	Any artefacts or remnants of the source subtraction process are incorporated into the RMS.	RMS	
Filtering	No additional uncertainties are introduced in this step.	Nil	
Calibration	There are no additional calibration steps, so no additional uncertainties are introduced.	Nil	
Calculation, Pre-processing at S&T			
Data Conversion	Input and output quantities have been verified to match to machine precision so no additional uncertainties are introduced in this step.	Nil	
Splitting by mode	Input and output quantities have been verified to match to machine precision so no additional uncertainties are introduced in this step.	Nil	
Calculation, Calibration at S&T			
Phase calibration	Any artefacts or remnants of the phase calibration process are incorporated into the RMS.	RMS	
Amplitude calibration	Not used in this measurement campaign	N.A.	
Distance proportionality	The spatial resolvability of the measurement campaign introduces some variance.	±0.26 dB	
Bandwidth	Incorporated directly into the L-formula, the uncertainty on this parameter is both static, and orders of magnitude smaller than the other parameters.	Negligible	
Outlier filtering	A reduction is the number of baselines available to use for imaging. Any effects are incorporated into the RMS.	RMS	

Name	Conclusion	Quantitative Impact	
		Vertical polarization	Horizontal polarization*
Polarisation leakage	Incomplete coupling between the transmitted polarisation and LOFAR's dipoles.	±1.0 dB	±1.0 dB
Calculation, Imaging at S&T			
Imaging algorithm effectiveness	The algorithm has been verified to be effective for imaging a known point source. The impact of the performance of the algorithm on uncertainties is incorporated into the output images, and their peak/RMS values.	N.A.	

*: if different from Vertical

<End of document>